J Mater Sci: Mater Med (2014) 25:2471–2480
DOI 10.1007/s10856-014-5277-2

Physical and mechanical characterisation of 3D-printed porous titanium for biomedical applications

Aouni El-Hajje · Elizabeth C. Kolos · Jun Kit Wang · Saeed Maleksaeedi · Zeming He · Florencia Edith Wiria · Cleo Choong · Andrew J. Ruys

Received: 1 May 2014 / Accepted: 11 July 2014 / Published online: 23 July 2014

Abstract The elastic modulus of metallic orthopaedic implants is typically 6–12 times greater than cortical bone, causing stress shielding: over time, bone atrophies through decreased mechanical strain, which can lead to fracture at the implantation site. Introducing pores into an implant will lower the modulus significantly. Three dimensional printing (3DP) is capable of producing parts with dual porosity features: micropores by process (residual pores from binder burnout) and macropores by design via a computer aided design model. Titanium was chosen due to its excellent biocompatibility, superior corrosion resistance, durability, osteointegration capability, relatively low elastic modulus, and high strength to weight ratio. The mechanical and physical properties of 3DP titanium were studied and compared to the properties of bone. The mechanical and physical properties were tailored by varying the binder (polyvinyl alcohol) content and the sintering temperature of the titanium samples. The fabricated titanium samples had a porosity of 32.2–53.4 % and a compressive modulus of 0.86–2.48 GPa, within the range of cancellous bone modulus. Other physical and mechanical properties were investigated including fracture strength, density, fracture toughness, hardness and surface roughness. The correlation between the porous 3DP titanium-bulk modulus ratio and porosity was also quantified.

A. El-Hajje · E. C. Kolos (✉) · A. J. Ruys
Biomedical Engineering, School of AMME, J07, University of Sydney, Sydney, NSW 2006, Australia
e-mail: elizabeth.kolos@hotmail.com

J. K. Wang · C. Choong
School of Materials Science and Engineering, Nanyang Technological University, 50 Nanyang Avenue, Singapore 639798, Singapore

S. Maleksaeedi · Z. He · F. E. Wiria
Singapore Institute of Manufacturing Technology, 71 Nanyang Drive, Singapore 638075, Singapore

1 Introduction

Titanium and titanium alloys have been widely used in orthopaedics in areas such as hip implants, cranioplasty, oral/maxillofacial repair and dental implants due to their high strength to weight ratio, superior corrosion resistance, excellent biocompatibility, durability, osteointegration capability and their relatively low elastic modulus [1–5]. In comparison to stainless steel (190 GPa) and cobalt-chrome (230 GPa), titanium (110 GPa) is considered a low modulus metal [6]. However, the modulus of titanium is still six times greater than cortical bone (7–30 GPa) [7, 8]. This can lead to a mismatch in Young's modulus creating a stress shielding effect. As a result, bone shielded from stress by the stiff metal implant atrophies and gradually loses its load bearing capability which can result in bone fractures at the implantation site [9]. In addition, the modulus mismatch between dense titanium and bone can lead to an unstable interface between bone and implant due to bone resorption during the bone remodelling process. To solve these problems and achieve longer implant life, researchers have investigated introducing a porous structure into the titanium implant to reduce the modulus of the material to closer match that of bone [10, 11]. Introducing pores into an implant will lower the modulus significantly [12]. Also, a metallic implant with a porous structure allows tissue to grow into it, which enables enhanced bonding between the implant and the bone [13].

To fabricate porous titanium, rapid prototyping (RP) has been utilised to efficiently generate titanium of desired properties. RP has the ability to control matrix architecture

such as size, shape, interconnectivity, branching, geometry and orientation, producing biomimetic structures that vary in design and material composition [14, 15].

The most common RP techniques used to fabricate porous titanium implants are selective laser melting (SLM), electron beam melting (EBM) and laser engineered net shaping (LENS) [4, 16]. SLM uses high power solid-state lasers to melt very fine metal powders in inert gas atmospheres [17]. The SLM technique enables the production of solid, dense metal parts. EBM parts are built through a directed solidification of the metal powder using a high energy electron beam gun in a vacuum which melts the metal powder one layer at a time [16, 18, 19]. LENS uses a laser which focuses onto a metal substrate to create a molten metal pool on the substrate. The metal powder is then injected into the liquid metal pool which melts and solidifies. The substrate is then scanned with respect to the laser head to write a metal line of finite width and thickness. Rastering of the part back and forth to create a pattern and fill material in desired areas allows a layer of material to be deposited [20]. Although these processes are well established for making customised titanium implants, the machinery is complicated and expensive.

In the present work, inkjet three dimensional printing (3DP) was used as a low cost RP technique that provides some unique advantages over other RP techniques for metals. Instead of using laser or electron beam to melt the powder, an ink cartridge was used to precision-print a fine water jet into a titanium-binder powder bed, layer by layer, according to a computer aided design (CAD) design. The resultant green (unsintered) titanium parts could be subsequently sintered in a furnace to obtain the necessary strength. The key advantages of inkjet 3DP are a much lower capital cost of the equipment and a capability to control the sintering process via the subsequent thermal cycle. Although precision of the parts made by inkjet 3DP is not as high as for SLM, EBM or LENS [21], for biomedical applications the precision of the parts made by 3DP is more than sufficient for the dimensional requirements. Therefore, inkjet 3DP is a suitable technique for low cost rapid manufacturing of biometallic components.

In this work, a study of the manufacturing and characterisation of porous titanium specimens using inkjet 3DP method is presented. The objective was to fine-tune the 3DP process to match the elastic modulus of the 3DP titanium with that of bone so as to eliminate stress shielding. Mechanical properties were investigated by tensile, compressive, three-point bending, and hardness testing. Physical properties such as density, porosity and surface roughness were investigated by mercury porosimetry and surface profilometry. These properties are then compared to the theoretical values of bone. Optimal mechanical properties were achieved by altering the two key independent variables: sintering temperature and binder content. A secondary objective was to quantify a correlation between 3DP titanium-bulk modulus ratio and porosity using predesigned porosity.

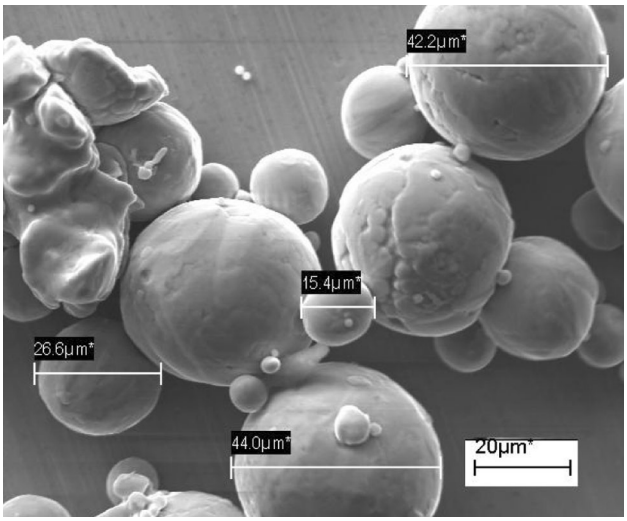

Fig. 1 SEM image of CP titanium powder

2 Materials and Methods

2.1 Materials

A commercially pure (CP) titanium powder grade 2 (supplied by TLS Technik GmbH & Co. Spezialpulver KG) was used with polyvinyl alcohol (PVA) (molecular weight of 320 g/mol) as the binder powder (supplied by The Nippon Synthetic Chemical Industry Co., Ltd., Japan). Two metal:binder ratios were investigated: 95:5 and 90:10 wt%. The SEM image in Fig. 1 exhibits the spherical nature of the titanium particles. Their average particle size was 45 µm.

2.2 Preparation of feedstock

Titanium powder and PVA binder were batched in the ratios of either 5 or 10 wt% PVA binder then dry ball milled in a polypropylene jar with 20 mm diameter zirconia balls for 24 h at a speed of 50 rpm to form a uniform well-mixed powder blend. The powder mixture was then dried using a vacuum oven for an hour at 60 °C to enhance the water absorption during printing. Lastly, the powder was sieved to filter out all the large particles (>180 µm) as well as removing all the agglomerates. A fine free-flowing powder bed is essential for efficient inkjet 3DP.

2.3 Printing and post processing

3DP was conducted in accordance with previous work by the authors [22]. A schematic diagram of the 3DP process is shown in Fig. 2. The titanium samples were first designed in a CAD environment using Solidworks software. The dried titanium/PVA powder mixture was then placed in the feeding chamber of the printer and spread evenly across the feeder and builder. During the printing process, the roller spread a layer of 0.1 mm thick powder onto the builder and the printer raster-printed the image via a fine water-jet onto the powder bed layer by layer. After the whole process was completed, the samples remained in the printer for an hour. This was to enable the water droplets enough time to disperse into the pores between the particles according to the printed shape and to allow time for the binder to air dry and strengthen the green part. This made it easier to handle during the de-powdering process. Figure 3 shows the printed green samples.

Once depowdered, the samples were placed into argon gas-filled furnace and heated slowly during the binder burnout temperature range, and then sintered at 1,250 or 1350 C (sintering time of 2 h), or 1,370 C (sintering time of 5 h). The binder acts as a porogen and produces the "pores by process", micron sized pores between each titanium particle, created during the binder burnout process. Pores by design (0.1 mm and larger) were engineered into the part by the printing process, which worked from a CAD file generated by SolidWorks software.

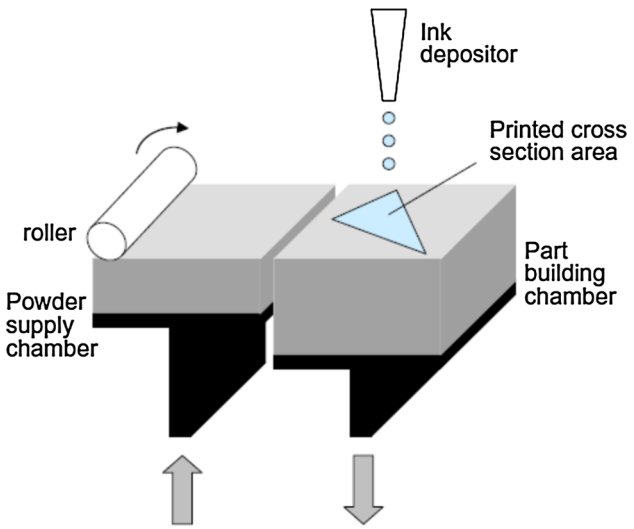

Fig. 2 Schematic of 3DP process

2.4 Characterisation methods

The physical properties were characterised by the Taylor Hobson-Form Talysurf Series 2 stylus profilometer machine to obtain surface roughness values, the Jeol JEM 5410 LV scanning electron microscope (SEM) to identify the microstructure, and Micromeritics AutoPore IV Mercury Porosimeter to obtain porosity, density and pore size.

Mechanical testing conducted included the tensile test according to ASTM E8/E8 M-11, compression test in accordance with ASTM E9-09 and three-point bending test according to ASTM E1820-11, conducted using an INSTRON Universal Testing Machine to obtain tensile modulus, fracture strength, compression modulus and fracture toughness. Rockwell hardness testing using the Indentec 8150SK Rockwell hardness tester was also performed on the titanium samples and bone in accordance with ASTM E18-08b. The bone used was a frozen femoral bovine bone obtained from an abattoir. Compression testing was also executed on the "pores by design" specimens.

3 Results and discussion

3.1 Physical properties of porous titanium (pores by process)

A summary of the physical properties of both samples with 5 % PVA and with 10 % PVA sintered at different temperatures is shown in Table 1.

The titanium sample with 5 % PVA binder sintered at 1,250, 1,350 or 1370 °C exhibited a porosity value in the range of 32.2–52.7 % with a median pore diameter of 20 μm whereas titanium with 10 % PVA binder under the same conditions displayed a porosity range of 44.5–53.4 %

Fig. 3 Green printed samples featuring compression bars, pores by design specimens, fracture toughness samples and tensile bars

Table 1 Physical properties of Ti specimens at different sintering temperatures

Testing	5 wt% PVA			10 wt% PVA		
	1,250 °C	1,350 °C	1,370 °C	1,250 °C	1,350 °C	1,370 °C
Porosity (%)	52.7	40.0	32.2	53.0	53.4	44.5
Median diameter (pores by process) (μm)	20.5	22.1	16.9	23.6	24.9	23.9
Density (g/cm^3)	2.5	2.9	3.1	2.3	2.9	2.8
Roughness Ra (μm)	20.7 ± 2.4	20.5 ± 1.8	22.3 ± 2.2	22.9 ± 4.2	23.5 ± 5.5	20.0 ± 2.4

One sample tested for porosity, median diameter and density only

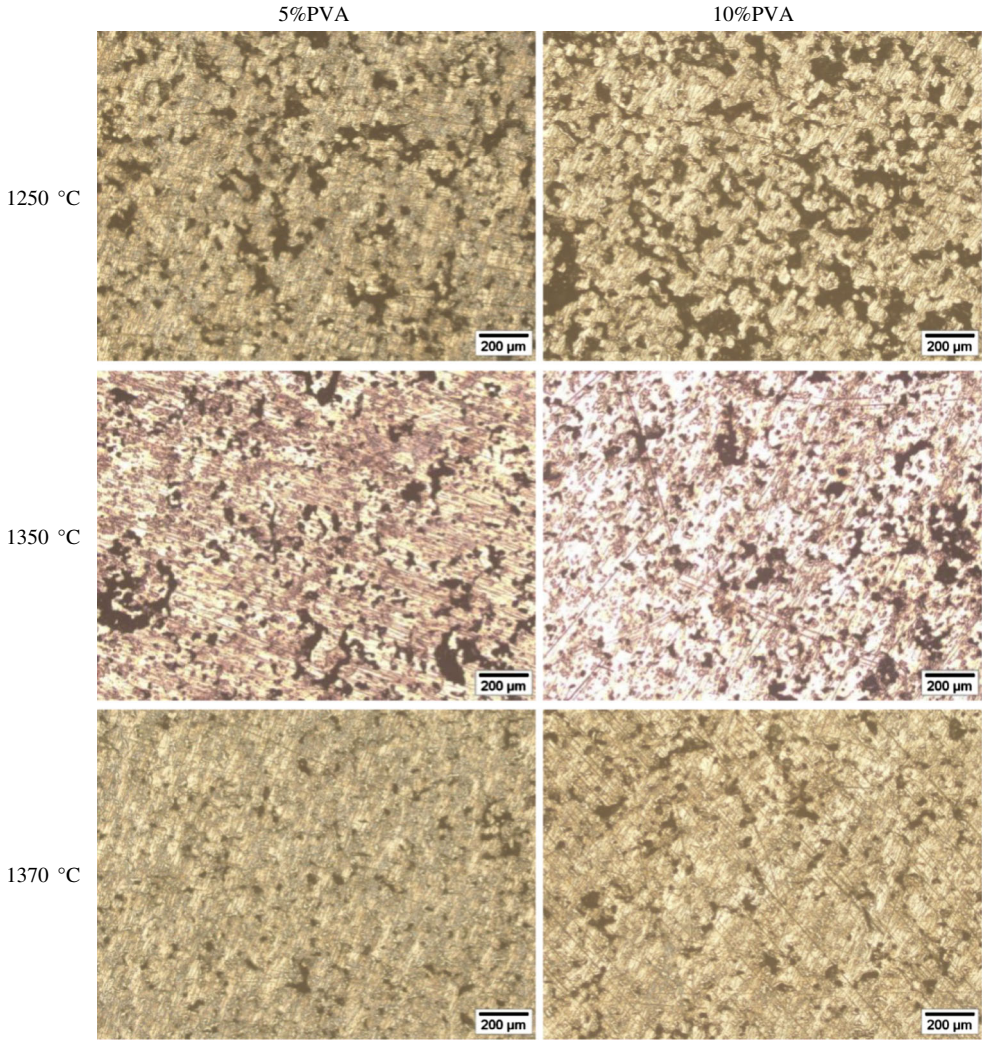

Fig. 4 Optical microscopy images of polished surfaces of Ti-5 % PVA (*left*) and Ti-10 % PVA (*right*) sintered at 1,250, 1,350 and 1370 °C "pores by process"

with a median pore diameter of 24 μm. Thus samples with 10 % binder presented a higher porosity and a greater pore size due to the amount of binder which acted as a porogen.

Optical microscopy images in Fig. 4 shows titanium samples with 5 and 10 % PVA binder sintered at 1,250, 1,350 and 1370 °C. Generally porosity is decreasing with increasing sintering temperature with greater porosity for titanium made with 10 % PVA. These results correlate with porosity measured by mercury porosimetry. Increasing sintering temperature is expected to reduce porosity due to further particles fusing. However, porosity measured for titanium made with 10 % PVA with 1,250 and 1350 °C was of a similar value. Visual observation made on optical microscopy suggests that samples sintered at 1,350 °C

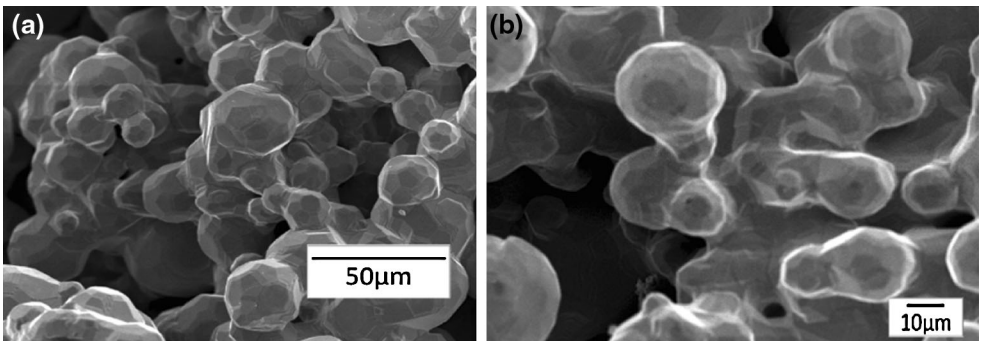

Fig. 5 SEM images of Ti-5 % PVA sintered at 1,250 °C showing **a** interconnected "pores by process" (magnified ×350), **b** an open "pore by process" (magnified ×750)

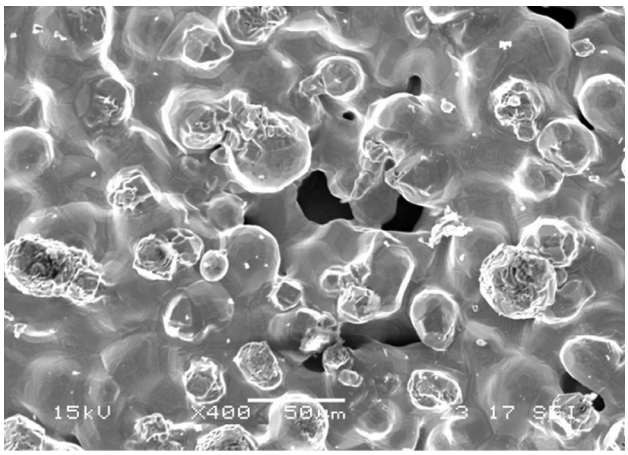

Fig. 6 Rough morphology of Ti-10 % PVA surface sintered at 1,350 °C (magnified ×400)

have less porosity than those sintered at 1,250 °C. This could be due to mercury not being able to penetrate the pores due to closed porosity.

The SEM images in Figs. 5a and b shows interconnected open pores which may assist cell attachment and in reducing the elastic modulus. Introducing pores into an implant will also lower the modulus significantly [10, 12, 23].

It was found that 3DP titanium made with 5 % PVA was denser than 3DP titanium made with 10 % PVA with density values of 2.5–3.1 g/cm^3 (5 %) compared with 2.3–2.9 g/cm^3 (10 %). The higher porosity of 3DP titanium made with 10 % PVA contributed to the resulting lower density. Increasing sintering temperature generally reduced porosity and generally increased density. Increasing sintering temperature from 1,350–1,370 °C did not significantly alter the density for titanium made with 10 % PVA.

The Stylus Profilometer revealed that 10 % PVA specimens generally exhibited a rougher surface than 5 % PVA specimens, with roughness values R_a of 20–23.5 μm for 10 % PVA as opposed to 20.5–22.3 μm for 5 % PVA. As the PVA binder increases, the surface roughness of the specimens could be expected to increase. This is due to poor stacking of the powder and low packing density due to different foreign particles composition. The increased surface roughness may enhance the bone-to-implant contact and assist cell attachment [24]. An SEM image showing the rough surface morphology is shown in Fig. 6.

3.2 Mechanical properties of porous titanium (Pores by process)

Table 2 summarises the mechanical properties of all 3DP test specimens. The results of ten specimens were averaged and tabulated. From the tensile test, 3DP titanium made with 5 % PVA and sintered at 1,370 °C produced an optimum outcome. It gave the best combination of high fracture strength, high compressive modulus, high fracture toughness, and high hardness. All specimens had a similar tensile modulus, within the range of about 5.5–8.5 GPa, which is at the low end of the normal range for cortical bone. This tensile modulus would minimize the effects of stress shielding and significantly reduce the chances of an implant loosening.

The tensile test was important to demonstrate that stress shielding would be minimised. It was also important to determine the compression modulus since many implants experience significant compressive loadings in vivo. Figure 7 shows the compression modulus of 3DP titanium made with 5 % and 10 % PVA and sintered at all three temperatures, for both pores by process and pores by design. 3DP titanium made with 5 % PVA and 1370 °C again produced an optimum outcome. The compressive modulus was just a little lower than the bottom end of the cortical bone range, and right at the top end of the cancellous bone range. As expected, the compressive modulus of the pores by process was significantly lower.

Table 2 Mechanical properties of Ti specimens at different sintering temperatures

Testing	5 wt% PVA			10 wt% PVA			Cortical bone
	1,250 °C	1,350 °C	1,370 °C	1,250 °C	1,350 °C	1,370 °C	–
Tensile modulus (GPa)	6.3 ± 0.9	7.1 ± 1.8	8.2 ± 0.8	5.6 ± 0.4	8.6 ± 3.0	6.9 ± 0.7	7–30 [7, 8]
Fracture strength (MPa)	78.8 ± 18.5	102.9 ± 31.8	245.7 ± 10.5	69.1 ± 14.1	125.2 ± 48.9	97.3 ± 27.2	79–194 [25]
Compressive modulus (GPa)	1.4 ± 0.2	2.2 ± 0.4	2.5 ± 0.2	0.9 ± 0.20	1.7 ± 0.30	2.1 ± 0.3	7–30 [7, 8]
Fracture toughness (MPa $m^{1/2}$)	5.5 ± 4.1	13.4 ± 4.5	16.9 ± 6.2	2.4 ± 1.6	7.0 ± 3.0	10.2 ± 3.7	3–10 [26]
Hardness (HRB)	18.1 ± 9.4	32.2 ± 15.3	33.5 ± 10.9	12.8 ± 4.2	21.6 ± 9.1	29.2 ± 10.6	32

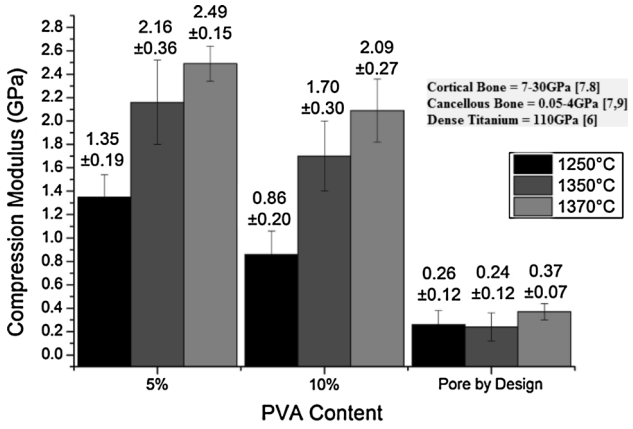

Fig. 7 Compression modulus of Ti specimens sintered at different temperatures

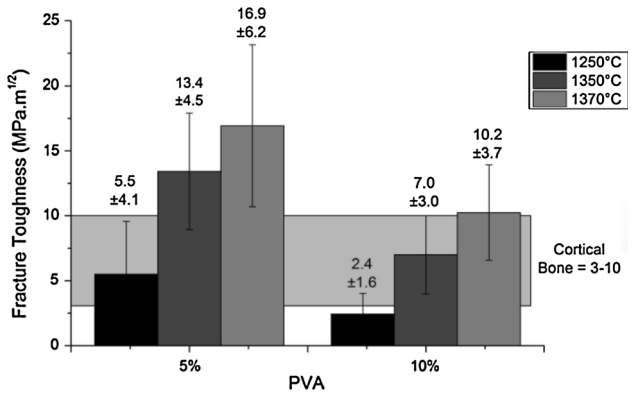

Fig. 8 Fracture toughness of Ti specimens sintered at different temperatures

The three-point bending test was used to obtain the fracture toughness of titanium samples. As noted before, 5 % PVA and 1,370 °C was the optimum, producing the highest fracture toughness value of 16.9 MPa $m^{1/2}$ which is significantly higher than cortical bone, which has a fracture toughness of 3–10 MPa $m^{1/2}$ [26]. Figure 8 shows the fracture toughness of 3DP titanium made with 5 and 10 % PVA and sintered at all three temperatures. 3DP titanium made with 5 % PVA had higher fracture toughness than that made with 10 % PVA at every sintering temperature. This was likely due to the lower porosity for 5 % PVA. The higher fracture toughness would be advantageous to provide a greater ability of the material to resist fracture when a crack is present.

Hardness values of titanium were obtained using the rockwell hardness machine. Again, 5 % PVA and 1,370 °C was the optimum which produced a maximum hardness of 33.5 HRB. Rockwell hardness was also tested on bone which gave a result of 32 HRB. Thus the 3DP titanium has an identical hardness to bone. The fracture strength of the 5 % PVA and 1370 °C was 245 MPa, the optimal outcome, and this was significantly higher than the reported range for cortical bone of 79–194 MPa [25].

Figure 9 shows SEM images of the fracture surfaces for titanium samples with 5 and 10 % PVA binder sintered at 1,250, 1,350 and 1,370 °C. SEM images shows that with increasing sintering temperature the appearance of the fracture surface becomes more flat. The portion of the fracture surface that real fracture (broken atomic bonds) has occurred occupies a very small area. The majority of what is seen is interconnected channels that have been exposed after fracture. Unlike dense materials, it is not easy to identify the start and end point of fracture in porous materials. Such materials have many defects in which fracture can initiate. In this case the weakest points are the necks between particles. This is likely to be the initiation point for crack propagation.

It was observed that generally tensile modulus, fracture strength, compression modulus, fracture toughness and hardness increased with sintering temperature. The exception was for tensile modulus and fracture strength at 10 % PVA and sintering at 1,350 °C.

It was possible that increasing sintering temperature resulted in carburisation of the carbon content of the PVA reacting with the titanium to form titanium carbide. Carbon content in metals is known to have an effect on improving mechanical properties. For example the modulus of TiC is approximately 460 GPa whereas titanium has a modulus of

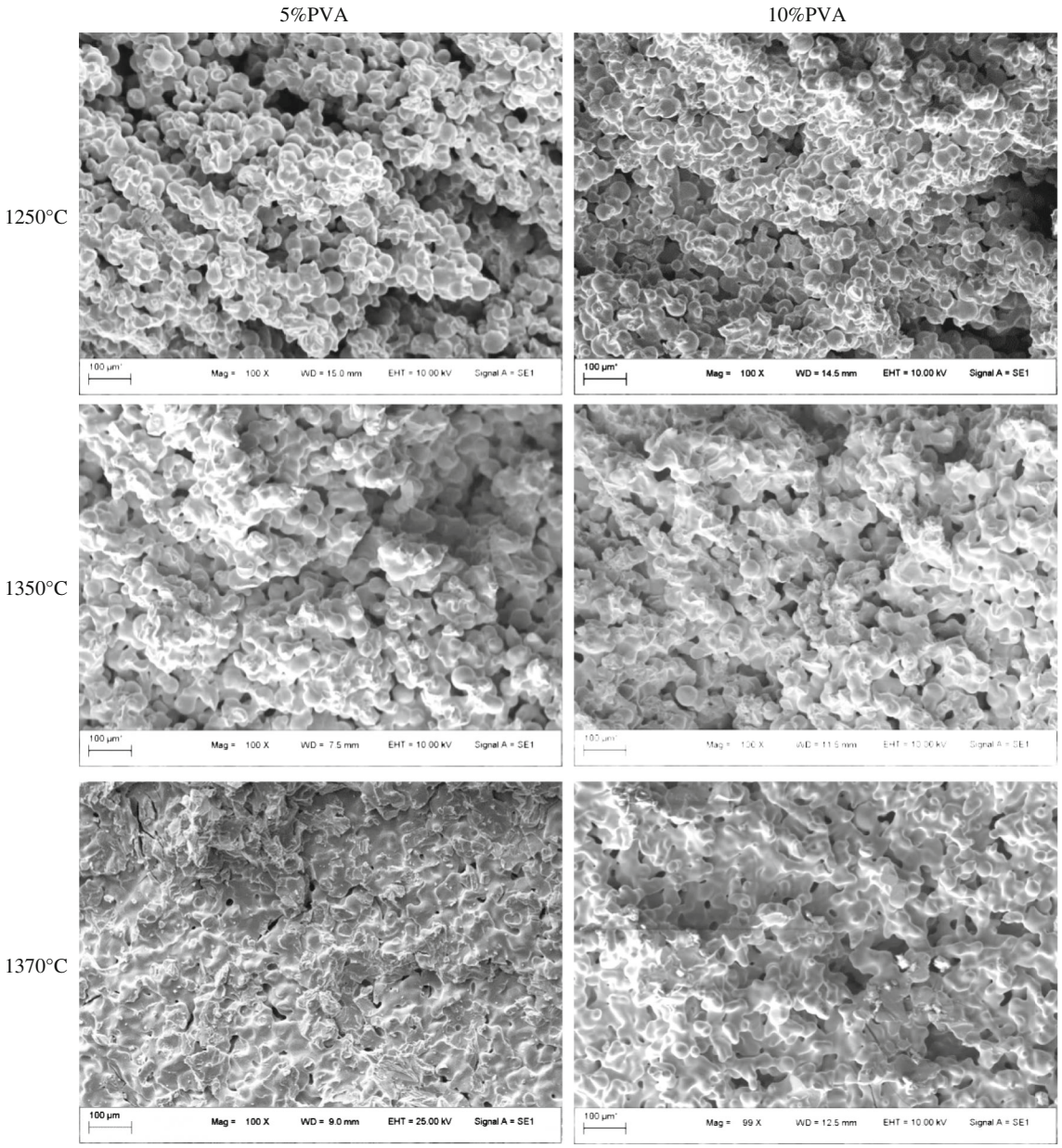

Fig. 9 SEM images of fracture surfaces of Ti-5 % PVA (*left*) and Ti-10 % PVA (*right*) sintered at 1,250, 1,350 and 1,370 °C "pores by process"

110 GPa [27]. TiC as a coating on titanium is also known to improve biocompatibility through surface stability and osseointegration through improved bone growth compared to titanium alone [28].

Titanium made with 10 % PVA and sintered at 1,350 °C had a higher tensile modulus and fracture strength than titanium made with 10 % PVA and sintered at 1,370 °C. A possible explanation is that increasing sintering temperature or sintering for longer at 1,370 °C reduced strength due to some oxidisation of the titanium occurring even though sintering was done in an argon gas-filled furnace. Oxidisation would continue at increasing sintering temperature and may have had an effect of the mechanical properties by making it more brittle. Grain growth may have also been a contributing factor.

In summary, 5 % PVA and 1370 °C was the optimum. It produced fracture toughness and fracture strength significantly higher than cortical bone, Rockwell hardness identical to bone, and the highest tensile and compressive modulus just less than the bottom end of the cortical bone range and at the top end of the cancellous bone range. Thus, the 3DP titanium is a good match for bone in terms

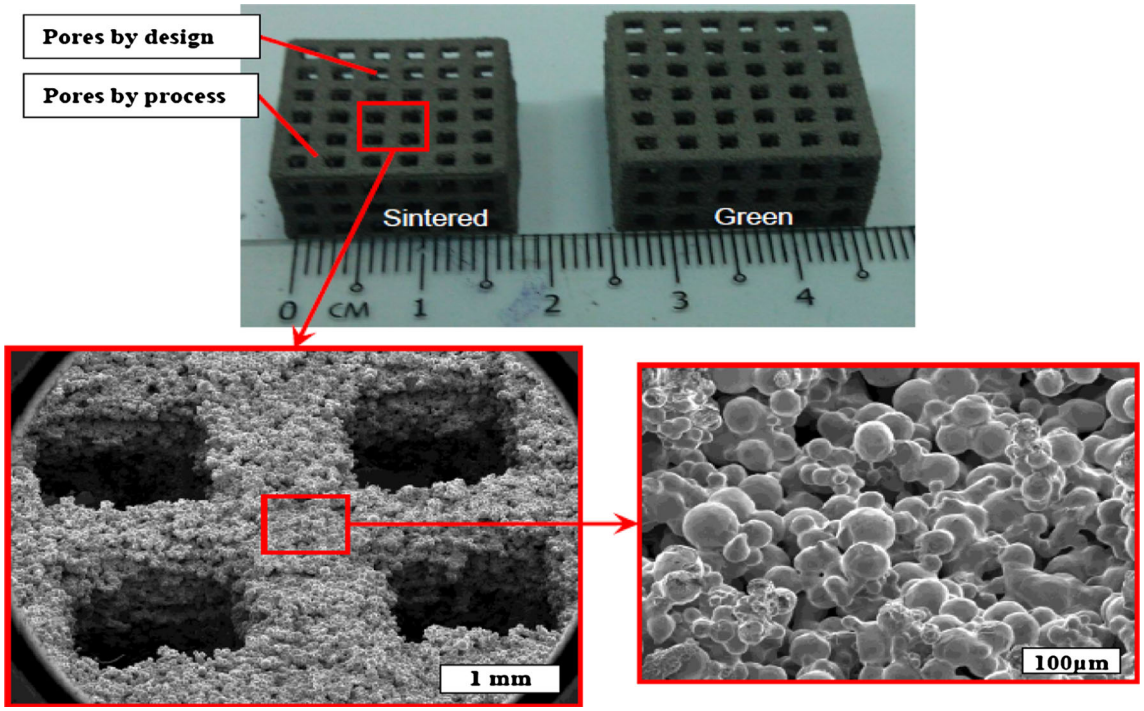

Fig. 10 Images of 3DP Titanium with pores obtained by engineering the manufacturing process "pores by design" (binder content 10 wt% sintered at 1,250 °C)

of stress shielding minimisation and overall mechanical integrity.

3.3 Mechanical properties of porous 3DP titanium with pre-designed porosity (pores by design)

The compression test was performed on porous 3DP titanium with "pores by design", i.e., pores generated obtained by engineering the manufacturing process through the CAD model. These specimens are shown in Fig. 10. The specimens had a pre-designed pore size of 2 mm and a wall thickness of 1.2 mm. A low compression modulus of 0.24–0.37 GPa was obtained which was well within the modulus range of cancellous bone (0.05–4 GPa) [7, 9].

An equation was formulated which linked the porous 3DP titanium modulus to the bulk modulus, wall thickness and pore size.Porous 3DP titanium modulus equation relating the bulk modulus, strut width between each pore (wall thickness) and pore width is given below.

$$E_S = E_B \times \left(\frac{W}{W+P}\right)^2 \quad (1)$$

E_s, modulus of porous 3DP titanium E_b, modulus of bulk titanium W, strut width between each pore;P, Pore widthA porosity equation was also derived which related the porosity to the wall thickness and pore size. The equation is:

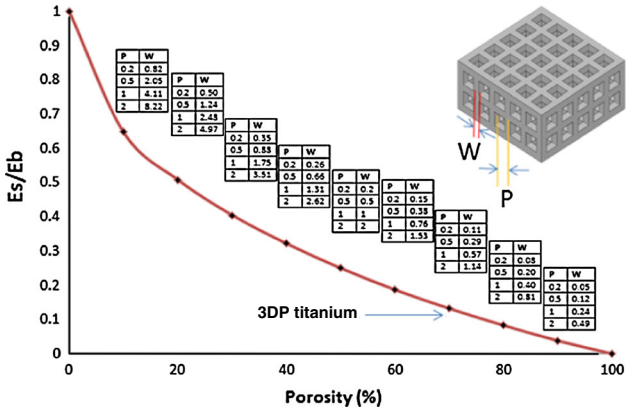

Fig. 11 Relationship between porosity and the porous 3DP titanium-bulk modulus (E_s/E_b) ratio. The desired porosity can be achieved by matching the modulus ratio with a certain pore size (P) and strut width between each pore (W)

$$\text{Porosity} = \frac{P^2(P + 3W)}{(P + W)^3} \quad (2)$$

The relationship between porosity and the porous 3DP titanium-bulk modulus (E_s/E_b) is shown in Fig. 11. This graph was generated by at random selecting pore size and wall thickness values and calculating the porosity using the above equations. Porous 3DP titanium modulus/bulk

modulus (E_s/E_b) ratio was calculated using pore size and wall thickness for validation of the equations.

The specimens had a pre-designed pore size of 2 mm (P = 2) and a wall thickness of 1.2 mm (W = 1.2). These two values were inserted into the above porosity equation and gave a porosity of 70 %. The porous 3DP titanium modulus from the compression test was approximately 0.3 GPa and the bulk modulus obtained from the compression test was approximately 2 GPa which gave a ratio of 0.15 which corresponds to approximately 70 % porosity. Therefore, the experimental results matched the theoretical results. In a typical example, using other rapid manufacturing methods such as EBM or SLM which produces dense metal parts, with a designed porosity of 60 %, the bulk modulus of titanium would be around 110 GPa and by interpolating the graph and conducting simple mathematics, a modulus of 22 GPa can be achieved which perfectly matches the modulus of bone, eliminating stress shielding.

4 Conclusion

CP titanium with PVA as the binder has been successfully investigated to fabricate 3D printed porous titanium samples for biomedical applications. The mechanical and physical properties were engineered by varying the two processing variables: sintering temperature and binder content.

The physical properties of porous 3DP titanium showed a porosity of 32.2–53.4 % (inherent porosity or "pores by process") with a median pore diameter of 20–24 μm. The porosity provides may assist cell attachment plus it reduces the elastic modulus. The density ranged from 2.3 to 3.1 g/cm^3 and a surface roughness of 20–23.5 μm was obtained.

The optimal specimens were produced with 5 % PVA binder and 1370 °C sintering temperature. These specimens were compared with known properties of bone. The specimens had a tensile modulus of 8.15 GPa which was within the range of bone, a fracture strength of 245.7 MPa which was higher than that of bone, a compressive modulus of 2.48 GPa that was within the range of cancellous bone, a fracture toughness of 16.9 MPa m$^{1/2}$ which was just higher than that of bone and a rockwell hardness of 33.5 that was the same as bone.

Compression tests on specimens with 2 mm pores by design produced a modulus of 0.3 GPa. A porous 3DP titanium modulus equation incorporating bulk modulus, wall thickness and pore size was generated and a porosity equation was also formulated. A porous 3DP titanium/bulk modulus ratio was plotted against porosity to show that pore size and wall thickness can be predesigned to obtain the desired porosity.

References

1. Hong SB, Eliaz N, Leisk GG, Sachs EM, Latanision RM, Allen SM. A new Ti-5Ag alloy for customized prostheses by three-dimensional printing (3DPTM). J Dent Res. 2001;80(3):860–3.
2. Oh I, Nomura N, Masahashi N, Hanada S. Mechanical properties of porous titanium compacts prepared by powder sintering. Scr Mater. 2003;49(12):1197–202.
3. Parthasarathy P, Starly B, Raman S, Christensen A. Mechanical evaluation of porous titanium (Ti6Al4V) structures with electron beam melting (EBM). J Mech Behav Biomed. 2010;3(3):249–59.
4. Laoui T, Santos E, Osakada K, Shiomi M, Morita M, Shaik SK, Tolochko NK, Abe F. Properties of titanium implant models made by laser processing. Proc Inst Mech Eng C J Mech Eng Sci. 2004;6:857–63.
5. Sollazzo V, Pezzetti F, Palmieri A, Girardi A, Farinella F, Carinci F. Genetic effects of trabecular titanium on human osteoblast-like cells (MG-63): An in vitro study. J Biomim Biomater Tissue Eng. 2011;9:1–16.
6. Srivastav A. In: Laskovski A, editor. An overview of metallic biomaterials for bone support and replacement. Moradabad: In-Tech; 2011.
7. Chandrasekaran M, Lim KK, Lee MW, Cheang P. Effect of process parameter titanium alloy fabricated using 3D printing. SIMTech Tech Rep. 2007;8(1):1–4.
8. Dewidar M, Mohamed HF, Lim JK. A new approach for manufacturing a high porosity Ti-6Al-4V scaffolds for biomedical applications. J Mater Sci Technol. 2008;24(6):931–5.
9. Nouri A, Hodgson PD, Wen C. In: Mukherjee A, editor. Biomimetic porous titanium scaffolds for orthopedic and dental applications. Victoria: InTech; 2010.
10. Shen H, Brinson LC. A numerical investigation of porous titanium as orthopedic implant material. Mech Mater. 2011;43(8):420–30.
11. Subramani K. Titanium surface modification techniques for implant fabrication—from microscale to the nanoscale. J Biomim Biomater Tissue Eng. 2010;5:39–56.
12. Bandyopadhyay A, Espana F, Balla VK, Bose S, Ohgami Y, Davies NM. Influence of porosity on mechanical properties and in vivo response of Ti6Al4V implants. Acta Biomater. 2010;6(4):1640–8.
13. Dabrowski B, Swieszkowski W, Godlinski D, Kurzydlowski KJ. Highly porous titanium scaffolds for orthopaedic applications. J Biomed Mater Res B. 2010;95(1):53–61.
14. Hutmacher DW. Scaffold design fabrication technologies for engineering tissues—state of the art and future perspectives. J Biomater Sci Polym Ed. 2001;12(1):107–24.
15. Subia B, Kundu J, Kundu SC. In: Eberli D, editor. Biomaterial scaffold fabrication techniques for potential tissue engineering applications. Kharagpur: InTech; 2010.
16. Abdelaal OA, Darwish SM. Fabrication of tissue engineering scaffolds using rapid prototyping techniques. WASET. 2011;59:577–85.
17. Bibb R. Medical modelling: The application of advanced design and development techniques in medicine. Cambridge: Woodhead Publishing Limited; 2006.
18. Parthasarathy J, Starly B, Raman S. A design for the additive manufacture of functionally graded porous structures with tailored mechanical properties for biomedical applications. J Manuf Process. 2011;13(2):160–70.
19. Petrovic V, Haro JV, Blasco JR, Portolés L. In: Lin C, editor. Additive manufacturing solutions for improved medical implants. Valencia: InTech; 2012.

20. Xue W, Krishna BV, Bandyopadhyay A, Bose S. Processing and biocompatibility evaluation of laser processed porous titanium. Acta Biomater. 2007;3(6):1007–18.
21. Leong KF, Cheah CM, Chua CK. Solid freeform fabrication of three-dimensional scaffolds for engineering replacement tissues and organs. Biomaterials. 2003;24(13):2363–78.
22. Wiria FE, Shyan JYM, Lim PN, Wen FGC, Yeo JF, Cao T. Printing of titanium implant prototype. Mater Des. 2010;31:S101–5.
23. Thelen S, Barthelat F, Brinson LC. Mechanics consideration for microporous titanium as an orthopedic implant material. J Biomed Mat Res. 2004;69A(4):601–10.
24. Rowe RC. The effect of the particle size of an inert additive on the surface roughness of a film-coated tablet. J Pharm Pharmacol. 1981;33(1):1–4.
25. Reilly DT, Burstein AH. The mechanical properties of cortical bone. J Bone Joint Surg. 1974;56-A(5):1001–22.
26. Ritchie RO, Buehler MJ, Hansma P. Plasticity and toughness in bone. Phys Today. 2009;62(6):41–7.
27. Török E, Perry AJ, Chollet L, Sproul WD. Young's modulus of TiN. TiC, ZrN and HfN. Thin Sold Films. 1987;153(1–3):37–43.
28. Brama M, Rhodes N, Hunt J, Ricci A, Teghil R, Migliaccio S, Della Rocca C, Leccisotti S, Lioi A, Scandurra M, De Maria G, Ferro D, Pu F, Panzini G, Politi L, Scandurra R. Effect of titanium carbide coating on the osseointegration response in vitro and in vivo. Biomaterials. 2007;28(4):595–608.